JOURNAL OF CATALYSIS 73, 257–271 (1982)

Studies of Carbon Monoxide Hydrogenation over Ruthenium Using Transient Response Techniques

NOEL W. CANT[1] AND ALEXIS T. BELL

Materials and Molecular Research Division, Lawrence Berkeley Laboratory, and Department of Chemical Engineering, University of California, Berkeley, California 94720

Received June 4, 1981; revised September 30, 1981

Transient response isotopic tracing was used together with *in situ* infrared spectroscopy to elucidate the dynamics of several elementary processes believed to occur during CO hydrogenation over ruthenium catalysts. Chemisorbed CO was observed to exchange very rapidly with gas phase CO and under reaction conditions the two species are in equilibrium. A similar conclusion was reached regarding the relationship between gas phase H_2 and adsorbed H atoms. The dissociation of molecularly adsorbed CO to form atomic carbon and oxygen was found to require vacant surface sites and to be reversible. It was shown that while CO is the principal adsorbed species present on the catalyst surface under reaction conditions, the catalyst also maintains a significant inventory of nonoxygenated carbon but no chemisorbed oxygen. It was also found that the rate at which nonoxygenated carbon undergoes hydrogenation is faster than the rate at which adsorbed CO is hydrogenated. This observation supports the hypothesis that the nonoxygenated carbon is an intermediate in CO hydrogenation.

INTRODUCTION

Ruthenium is a particularly interesting Fischer–Tropsch catalyst, since unlike iron and cobalt it does not form bulk carbides under reaction conditions and thus reactions proceeding on its surface can be studied in the absence of concurrent bulk processes. It is known from infrared measurements (*1–4*) that under normal reaction conditions in CO/H_2 mixtures ruthenium surfaces are covered with a near complete layer of carbon monoxide molecules. However, recent evidence from several groups (*3, 5–8*) suggests that an additional form of nonoxygenated carbon is also present and that the synthesis of methane and higher hydrocarbons proceeds by hydrogenation of this material. Perhaps the most convincing evidence for this view has been provided by Biloen *et al.* (*6*). They found that if nickel, cobalt, or ruthenium surfaces were partially covered by carbon in the form of ^{13}C by the Boudouard reaction of ^{13}CO and the undissociated ^{13}CO molecules were replaced by ^{12}CO molecules at 383 K, then a subsequent batch reaction in $^{12}CO + H_2$ resulted in incorporation of ^{13}C in similar proportions in all hydrocarbons. Araki and Ponec (*9*) and Wentrcek *et al.* (*10*) have also presented evidence for such conversion of surface carbon on nickel under non-steady-state conditions. In this laboratory Ekerdt and Bell (*3*) found that substantial carbonaceous material was laid down on a ruthenium catalyst under steady-state conditions and that its subsequent hydrogenation in the absence of gas phase CO proceeded with transient rates vastly in excess of steady-state rates.

There has been some debate as to whether the slow step in methane synthesis under steady-state conditions is carbon monoxide dissociation or some later step.

[1] Permanent address: School of Chemistry, Macquarie University, New South Wales, Australia.

0021-9517/82/020257-15$02.00/0

Dalla Betta and Shelef (*11*) favored the former on the grounds that it was consistent with absence of a significant kinetic isotope effect when D_2 was substituted for H_2. However, Wilson (*12*) pointed out that this evidence is not overwhelming since negligible kinetic isotope effects can result from compensating kinetic and thermodynamic effects. Recently, Kellner and Bell (*13*) reported that an inverse isotope effect is observed during synthesis over Ru/Al_2O_3. Both the nature and magnitude of the effect could be explained in terms of a scheme in which the slow step is the reductive elimination of a surface methyl group. All steps preceding this were assumed to be at equilibrium. More recently, Kellner and Bell (*14*) have also shown that the same scheme provides a satisfactory explanation of the kinetics of methane synthesis over Ru.

The purpose of the present work was twofold. First, to see if the conclusions of Biloen *et al.* (*6*), regarding the presence of reactive carbon, remained valid under steady-state conditions and, second, to establish relative rates for some of the individual steps in the scheme of Kellner and Bell (*13, 14*). The experiments involved a combination of isotopic labeling and rapid response mass spectrometery to monitor product formation while changes in surface species were followed on a similar time scale using Fourier-transform infrared spectroscopy.

EXPERIMENTAL

The experimental apparatus used has been described in detail in Ref. (*15*). The major flow system consisted of four separate gas supplies regulated by electronic flow controllers. One provided an Ar carrier flow into which any two of the three other supplies (normally CO, H_2, and Ar) were switched via four-way valves. The arrangement was such that no dead volumes existed but, depending on the individual flow rates, delays of up to 5 s occurred before the step change corresponding to a valve switch progressed to the reactor. A portion of the product stream from the reactor was sampled through a differentially pumped inlet system (*15*) into a vacuum chamber containing an EAI 250B quadrupole mass spectrometer. The latter was controlled by a microprocessor which fed the intensities of up to 11 mass spectrometer peaks per second to a data acquisition system for storage on magnetic tape. All information corresponding to a given experiment was retrieved and then plotted on an $X-Y$ recorder.

The reactor used for these studies was similar to that described by Hicks *et al.* (*16*). It consisted of two UHV flanges bolted together. Each flange was machined to accept a 25-mm-diameter CaF_2 window sealed in place with Graphoil gaskets. The catalyst sample consisted of a thin 20-mm-diameter pressed disk supported in a small aluminum holder which fitted into the 9-mm path length space between the windows. The temperatures, as recorded by a thermocouple in the gas flow close to the sample, was maintained constant to ± 1 K by external flat plate heaters controlled by an electronic temperature controller. With reactant gases flowing through it, the reactor approximated a CSTR with a calculated residence time in the range 0.6–3.5 s under the conditions used here.

The effective aperature for the windows of the reactor was 16 mm as required to take the circular beam of a Digilab FTS 10M Fourier-transform infrared spectrometer. Spectra of the disk of catalyst under reaction conditions were recorded with a resolution of 4 cm^{-1} requiring about 1.8 s to acquire each interferogram. Most spectra shown here were obtained from two successive interferograms coadded and stored on tape for later computation. This allowed spectra to be obtained at intervals down to 7 s. Spectra were computed and plotted in absorbance form as the ratio $\ln(I_r/I_s)$, where I_r represents a single beam spectrum of the disk after reduction in H_2 alone and I_s the sample single beam spectrum under some other condition.

A 4.3% Ru/SiO_2 catalyst was prepared by impregnating CAB-O-SIL HS-5 with an aqueous solution of $RuCl_3 \cdot 3H_2O$. The slurry was freeze-dried and then reduced for 2 hr in flowing H_2 at 673 K. The dispersion of the catalyst was determined from an H_2 isotherm obtained at 373 K and was established to be 0.22. Prior to use the catalyst was sieved and 50 mg of the −30, +60 mesh fraction was pressed into a self-supporting wafer.

High-purity argon (Liquid Carbonic) was obtained from cylinders with a stated oxygen impurity of <3 ppm. However, imperfections in the sealing of the windows led to a typical oxygen content of 10 ppm under reaction conditions. Hydrogen with a stated O_2 content <2 ppm was used. The carbon monoxide was Matheson Grade U.H.P. (99.8%). The D_2 used was from Liquid Carbonic and contained 2.8% HD. $^{13}C^{16}O$ and $^{12}C^{18}O$ were also obtained from Liquid Carbonic. The only significant impurity in the latter was 1% $^{12}C^{16}O$, but the former contained nearly 8% $^{13}C^{18}O$ and about 2% $^{12}C^{16}O$. All gases were used without purification.

RESULTS AND DISCUSSION

The experiments carried out fall into two classes—those in which the chemical composition of the adsorbed layers remain constant and those in which transients corresponding to changes in chemical composition were followed. Those of the former type will be described first.

Isotopic Exchange of Carbon Monoxide

This process was found to be rapid as may be seen from the spectra of Fig. 1, which illustrates replacement of adsorbed $C^{16}O$ by $C^{18}O$ at 323 K. At this temperature, the spectrum of the sample equilibrated with $C^{16}O$ (Fig. 1a) showed an intense absorption band at 2048 cm^{-1} due to carbon monoxide linearly adsorbed on surface ruthenium atoms (*1–4*). The corresponding absorption band for $C^{18}O$ was at 2004 cm^{-1} (Fig. 1c). The spectrum recorded

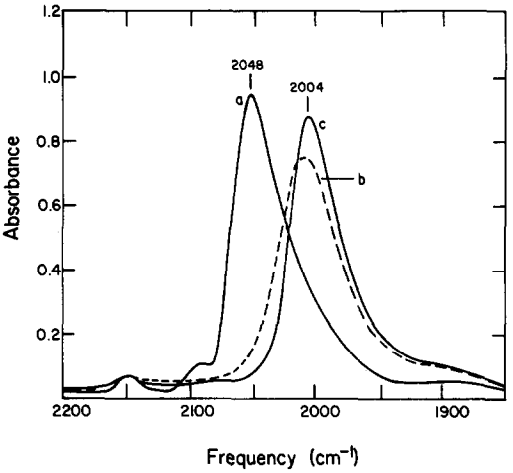

FIG. 1. Infrared spectra replacement of $C^{16}O$ adsorbed on Ru/SiO_2 by $C^{18}O$ at 323 K: P_{CO} = 28 Torr; P_{H_2} = 109 Torr; total flow rate = 4.86 STP cm^3/s. (a) in $C^{16}O$ alone; (b) 8 s after switching to $C^{18}O$; (c) 150 s after switching to $C^{18}O$.

8 s (Fig. 1b) after the input carbon monoxide was changed from $C^{16}O$ to $C^{18}O$ showed that the surface replacement process was already far advanced. At that time the gas phase was calculated to be about 90% $C^{18}O$ while the surface layer was greater than 80% $C^{18}O$. Estimates of the isotopic distribution in the adsorbed CO layer during isotopic exchange were achieved by reference to the calibration spectra shown in Fig. 2. These spectra were taken with $C^{16}O/C^{18}O$ mixtures of known composition.

It should be noted that the spectra of the isotopically mixed adsorbed carbon monoxide never corresponded to simple addition of the spectra of the individual components in proportion to their amounts present. This may be clearly seen in Fig. 2 where the spectrum with the greatest half-width and smallest absorbance did not correspond to a near equimolar mixture of $C^{16}O$ and $C^{18}O$ as one might expect, but rather to one in which the ratio of $C^{18}O/C^{16}O$ is about 3 : 1. This effect is well known for carbon monoxide adsorbed on both supported platinum particles (*17*) and platinum single crystals (*18, 19*). As first explained by Hammaker *et al.* (*17*), it arises

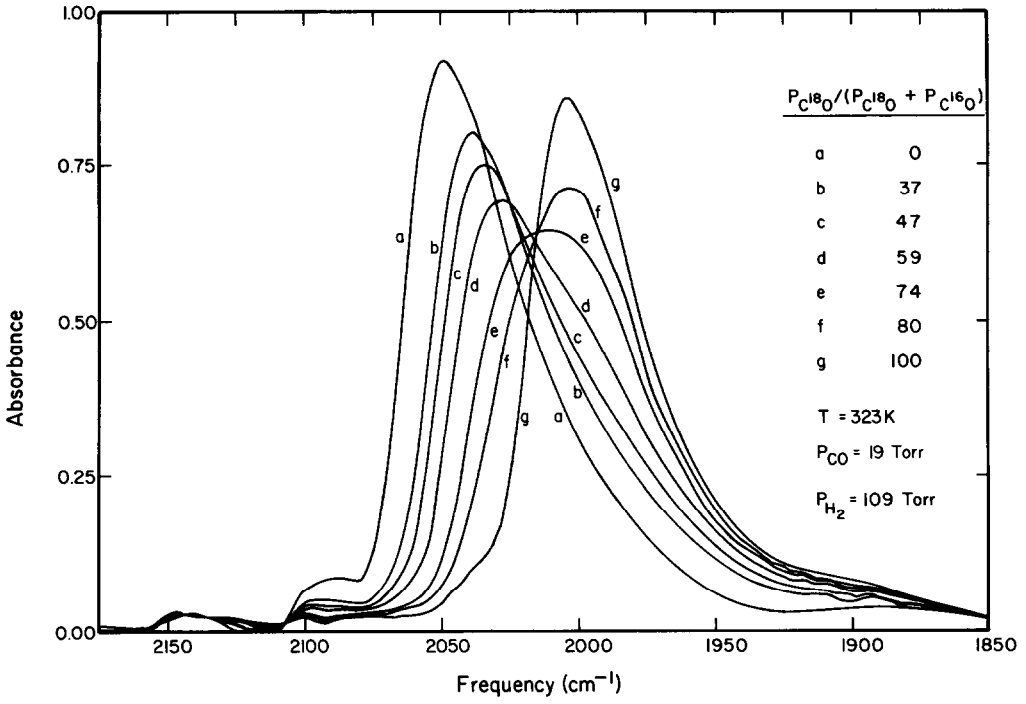

FIG. 2. Infrared spectra of Ru/SiO_2 in equilibrium with various mixtures of $C^{16}O$ and $C^{18}O$ at 323 K: P_{CO} = 28 Torr, P_{H_2} = 109 Torr; total flow rate = 4.86 STP cm^3/s.

as a result of dipole coupling in the adsorbed layer. Since the extent of coupling may vary with total coverage, and/or the presence of other species in the adsorbed layer, the only satisfactory way of obtaining surface composition from spectra of mixed isotopic layers is by direct comparison with spectra corresponding to known compositions under similar conditions.

In an attempt to follow the dynamics of the exchange process an exeriment was run at 300 K in the absence of H_2. The replacing gas was ^{13}CO at a low flow such that the change in isotopic composition in the gas phase could be monitored with the mass spectrometer while the surface composition was estimated from spectra recorded at 7-s intervals. The results are plotted in Fig. 3. The surface composition appears to lag about 2 s behind that of the gas phase but this delay may have been due in part to small systematic errors in timing. Thus, the desorption probability for adsorbed carbon monoxide molecules under these conditions must be equal to or greater than the gas phase space velocity, ~0.5 s^{-1}.

The very rapid exchange of chemisorbed CO with gas phase CO at low temperature reported here has been noted previously by Klier *et al.* (*20*) for Ni(110) and more re-

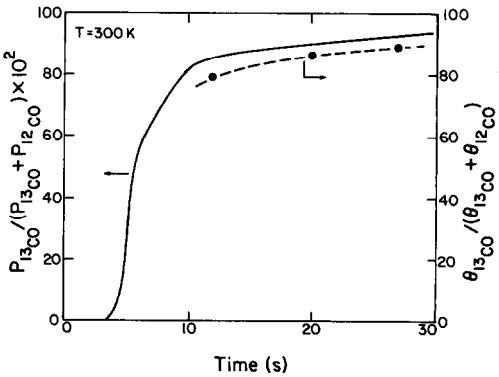

FIG. 3. Exchange of ^{12}CO adsorbed on Ru/SiO_2 by ^{13}CO at 300 K: P_{CO} = 11 Torr; P_{H_2} = 0.0 Torr; total flow rate = 3.2 STP cm^3/s.

cently by Yates *et al.* (*21, 22*) for silica-supported Rh and Ni(100). Yates *et al.* (*22*) proposed that the rapidity of the exchange could be explained by the population of low-adsorption energy states at high CO coverages. Rapid equilibration of the CO in these states with CO adsorbed in higher energy states would account for the exchange of the entire CO adlayer.

A significant question is whether the dynamics of exchange can be explained on the basis of the rate parameters for CO desorption from Ru in the literature. Pfnür *et al.* (*23*) have reported desorption parameters for CO adsorbed on Ru(001). Their data indicate that at maximum coverage the preexponential is less than 10^{15} s^{-1} and the activation energy is greater than 25 kcal/mole. Using these numbers, a desorption rate of less than 5×10^{-4} s^{-1} would be predicted at 300 K. This rate is significantly smaller than that observed in the present work. More recently, Kellner and Bell (*4*) have established from *in situ* infrared observations that the coverage of a Ru/Al_2O_3 catalyst by CO under synthesis conditions depends only on the CO partial pressure and can be described by a Langmuir isotherm. The adsorption equilibrium constant determined from these experiments is $K = 1.1 \times 10^{-9} \exp(25{,}500/RT)(atm^{-1})$. The rate coefficient for desorption, k_d, can be expressed as $k_d = k_a/K$, where k_a is the rate coefficient for adsorption. The value of k_a is given by

$$k_a = \frac{s_0}{RT}\frac{v_r}{4}, \qquad (1)$$

where s_0 is the sticking coefficient for CO at zero coverage, v_r is the random velocity for CO, and T is the gas temperature. Assuming $s_0 = 1.0$, the value of k_d at 300 K is determined to be 0.6 s^{-1}. This number is in very close agreement with the lower limit for k_d, 0.5 s^{-1}, deduced from the data presented in Fig. 3.

Comparison of the desorption parameters obtained by Pfnür *et al.* (*23*) and Kellner and Bell (*4*) indicates that while the activation energies for desorption reported by both sets of authors are nearly identical, the preexponential factor determined from Kellner and Bell's results is a factor of 10^3 larger than that reported by Pfnür *et al.* The reason for this substantial difference is not well understood at present. One possibility is that supported Ru catalysts expose a variety of surface planes in addition to the (001) surface and that the preexponential factors for desorption are significantly different on different planes. A second possibility is that the maximum adsorbate coverage attainable in the presence of several Torr or more of CO is greater than that achieved during adsorption at the pressures typically used for surface science studies (i.e., $\leq 10^{-4}$ Torr) and that the preexponential for desorption at very high coverages is greater than that observed for maximum coverage at low pressures. In this connection we note that the maximum ratio of CO to surface Ru atoms obtained by Pfnür *et al.* (*24*) on Ru(001) is reported as 0.7, whereas ratios in excess of 0.8 were found in the present work.

Isotopic Scrambling of $^{13}C^{16}O$ and $^{12}C^{18}O$

The rate of this process was ascertained by flowing a near equimolar mixture of $^{13}C^{16}O$ and $^{12}C^{18}O$ over the catalyst and examining the effluent stream for changes in the amounts of $^{12}C^{16}O$ and $^{13}C^{18}O$. Results obtained at 555 K (which approaches the maximum temperature continuously usable with the apparatus) are shown in Table 1. In the presence of 164 Torr of H_2, which resulted in 16% conversion of the inlet carbon monoxide flow, less than 1 molecule in 40 underwent mixing. When the flow of H_2 was shut off the extent of exchange increased over a period of 20 min to approximately 1 molecule in 20. Thus it is apparent that the rate of methane formation from CO and H_2 over ruthenium proceeds substantially faster than the rate of isotopic scrambling between $^{12}C^{18}O$ and $^{13}C^{16}O$.

The present observations are qualitatively consistent with those of Bossi *et al.*

TABLE 1

Isotopic Exchange Between $^{13}C^{18}O$ and $^{12}C^{18}O$ over Ru/SiO_2 at 555 K[a]

Mixture	$^{13}C^{18}O$ (%)	$^{12}C^{18}O$ (%)	$^{13}C^{16}O$ (%)	$^{12}C^{16}O$ (%)
Inlet	4.9	50.4	43.2	1.4
Exit (H_2 present)[b]	5.3	50.1	41.8	2.7
Exit (H_2 absent)	6.3	49.1	40.9	3.6

[a] P_{CO} = 23 Torr, total flow rate = 1.5–1.9 STP cm^3/s.
[b] P_{H_2} = 164 Torr, conversion of CO to $CH_4 \approx 16\%$.

(*25*). These authors observed that at 423 K isotopic exchange proceeded very slowly over a Ru/SiO_2 catalyst. By contrast, the rate of exchange occurred much more rapidly over a Ru/Al_2O_3 catalyst, but was severely inhibited in the presence of hydrogen.

Isotopic exchange can be envisioned to occur via the following mechanism

$$(1)\ {}^{12}C^{18}O \overset{+S}{\rightleftarrows} {}^{12}C^{18}O_s \overset{+S}{\rightleftarrows} {}^{12}C_s + {}^{18}O_s,$$

$$(2)\ {}^{13}C^{16}O \overset{+S}{\rightleftarrows} {}^{13}C^{18}O_s \overset{+S}{\rightleftarrows} {}^{13}C_s + {}^{16}O_s,$$

$$(3)\ {}^{12}C_s + {}^{16}O_s \overset{-S}{\rightleftarrows} {}^{12}C^{16}O_s \overset{-S}{\rightleftarrows} {}^{12}C^{16}O,$$

$$(4)\ {}^{13}C_s + {}^{18}O_s \overset{-S}{\rightleftarrows} {}^{13}C^{18}O_s \overset{-S}{\rightleftarrows} {}^{13}C^{18}O.$$

This reaction sequence is consistent with the fact that adsorbed CO is the predominant surface species observed under all conditions (*1–4*), and, as shown below, that for CO dissociation to produce atomic carbon requires vacant sites on the metal surface. Evidence from studies of CO disproportionation over ruthenium catalysts suggest that while CO dissociation is an activated process, the rate at which this reaction occurs at 473 K is significantly greater than that for isotopic scrambling (*6*). The recombination of adjacent carbon and oxygen atoms to form CO should be even more rapid than CO dissociation since recombination is an exothermic process (*26*). As a consequence it may be argued that neither CO dissociation nor the recombination of adjacent C and O atoms should limit the rate of isotopic scrambling. It is conceivable, however, that the rate-limiting step may be the surface diffusion of the atomic species. The inhibition of scrambling by the presence of hydrogen could be explained by the removal or surface oxygen to form water, thereby reducing the rate at which carbon and oxygen atoms can recombine.

Isotopic Scrambling of H_2 and D_2

This process was studied in a similar way to that with carbon monoxide by using H_2/D_2 mixtures and measuring HD formation. The results are given in Table 2. At 374 K in the absence of carbon monoxide equilibration was essentially complete. The presence of 36 Torr of carbon monoxide reduced HD formation to about 45% of equilibrium but the latter was restored by raising the temperature to 432 K or higher. Infrared spectra taken under the latter conditions showed that the near complete coverage of the catalyst surface by adsorbed CO was indistinguishable from that at 323 K. It is clear, however, that even at such high CO coverages H_2 and D_2 adsorption and dissociation are not impeded.

The mechanism of H_2/D_2 exchange over transition metal catalysts has been discussed at some length in the literature [see, for example, Ref. (*27*)]. It is now generally

TABLE 2

Isotopic Exchange between H_2 and D_2

P_{CO} (Torr)	Temperature (K)	H_2 (%)	HD (%)	D_2 (%)	Equilibration (%)
(Inlet mixture)	—	50	1	49	nil
nil	374	26	49	25	>95
36	374	39	22	39	45
36	432	26	49	25	>98

[a] $P_{H_2} + P_{D_2}$ = 107 Torr; total flow rate = 2.0 STP cm^3/s.

accepted that above room temperature exchange proceeds via the Bonhoeffer–Farkas mechanism which involves the dissociative adsorption of H_2 and D_2 and HD formation by recombination of H and D atoms. Implicit in this scheme is the reversibility of hydrogen chemisorption. Based on this background, it may be concluded that the observation of equilibrium H_2/D_2 exchange in the present study indicates that atomically adsorbed hydrogen is in equilibrium with hydrogen in the gas phase.

Transient and Steady State Formation of Methane and Water

The left half of Fig. 4 shows the response of mass spectrometer peaks with m/e = 15 (due to CH_3^+ from CH_4) and 18 (due to H_2O^+) to the addition and subsequent deletion of CO to a stream of H_2 and Ar flowing over the catalyst at 498 K. Addition of CO resulted in a small overshoot in CH_4 and H_2O production. Within 30 s, a steady rate of 10^{-8} mol CH_4 s^{-1} (equivalent to a turnover frequency per surface Ru atom of about 2.65×10^{-3} s^{-1}) was reached and this declined little over 3 min. Subsequent deletion of the CO component gave rise to substantial transient methane production with a peak rate exceeding five times the steady-state value. Water production exhibited a similar time dependence but the maximum rate was much lower. The relative sensitivity of the mass spectrometer to water and methane could not be exactly determined but was fairly close to unity as judged by the near equal intensities of the peaks for these components during steady-state reaction. Cumulative H_2O formation over the first 200 sec of the transient was about 3.0 μmol compared to 4.9 μmol for CH_4. The difference requires that while water may be produced from adsorbed carbon monoxide alone at least part of the methane must arise from another nonoxygenated carbon source.

For two reasons associated with the known inverse dependence of methane pro-

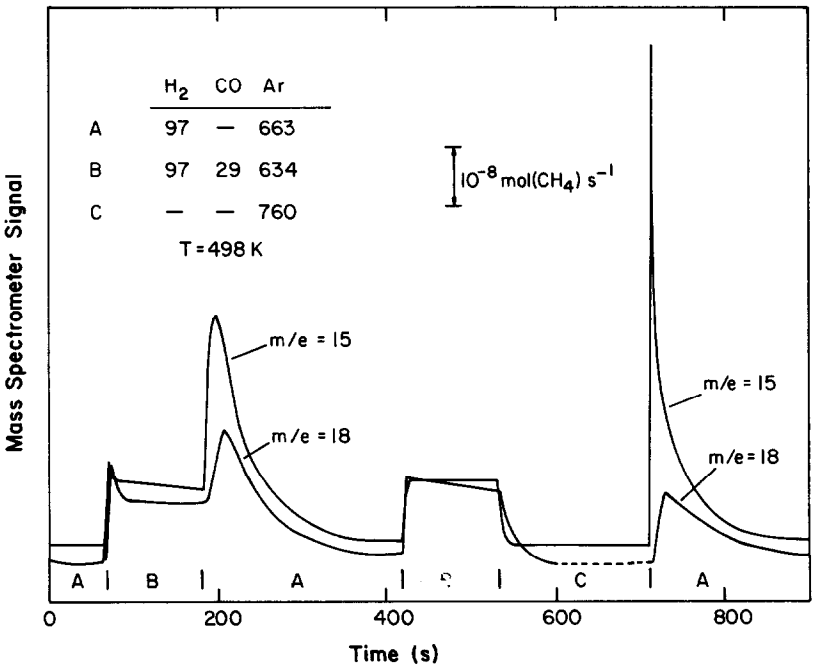

FIG. 4. Steady-state and transient formation of methane and water at 498 K: Total flow rate = 1.41 STP cm^3/s.

duction on CO pressure (*2, 14, 28–30*) it was felt that the shape of the methane transient described above might be determined in part by the fact that the pressure of residual CO takes some seconds to decline to a negligible value. First, the initial rise in methane production could be limited by the inability of H_2 to chemisorb in competition with residual CO and, second, since the rate would accelerate during the CO pressure decline, at least part of the methane and water produced could arise from reaction of some of the gas phase CO in the reactor (about 3 μmol). For this reason, a similar experiment was carried out in which a flushing period in Ar alone was introduced between the reaction mixture and subsequent exposure to H_2 in Ar. The results are shown in the right half of Fig. 4. The initial rise in methane production was dramatically sharper and in fact could be barely followed with the one point per second sampling of the mass spectrometer. On the other hand, transient water formation exhibited a time evolution similar to that shown before but cumulative production was less. Infrared spectra taken concurrently showed that this was attributable to loss of adsorbed CO during the argon flushing period. The amounts of methane and water produced in this experiment were 3.2 and 1.6 μmol, respectively.

Experiments of the above type demonstrated that some methane produced as a consequence of the step change CO + H_2 → Ar(20 s) → H_2 was being produced from a source of reactive nonoxygenated carbon. The quantity involved could be more accurately assessed by employing sequences such as $^{13}CO + H_2 \rightarrow {}^{12}CO + H_2$ (~ 30 s) → Ar(30 s) → H_2. Under appropriate conditions the short period in $^{12}CO + H_2$ produced a situation in which adsorbed carbon monoxide molecules were exclusively ^{12}CO whereas other carbon sources were ^{13}C. Subsequent transient production of $^{12}CH_4$ and $^{13}CH_4$ could be estimated from intensities of the mass spectrometer peaks with m/e = 15 and 17, respectively, after imposition of appropriate corrections. Results for one such experiment, at 463 K and including an intervening argon flush, are plot-

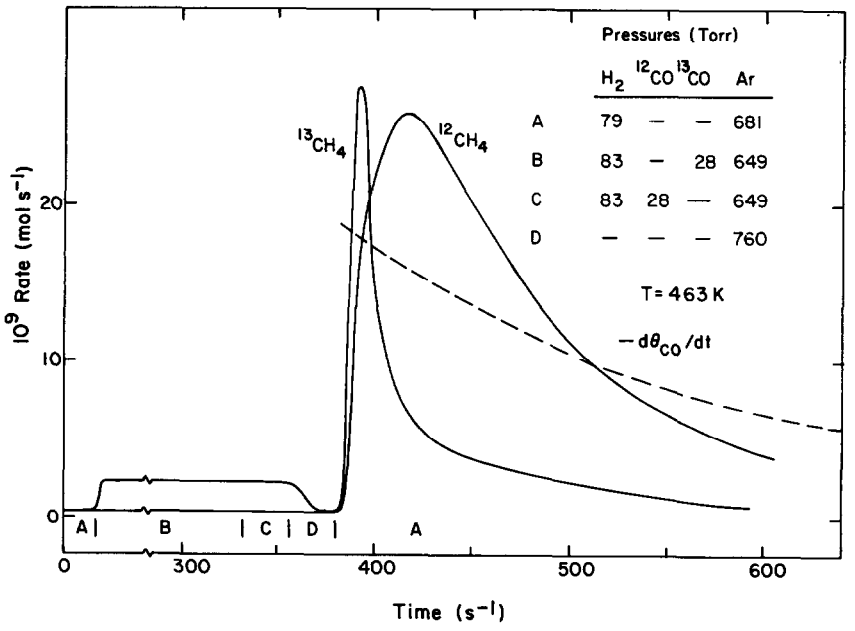

FIG. 5. $^{12}CH_4$ and $^{13}CH_4$ formation and loss of adsorbed ^{12}CO during the sequence $H_2 \rightarrow {}^{13}CO + H_2 \rightarrow {}^{12}CO + H_2$(30 s) → Ar(20 s) → H_2 at 463 K: Total flow rate = 0.85 STP cm³/s.

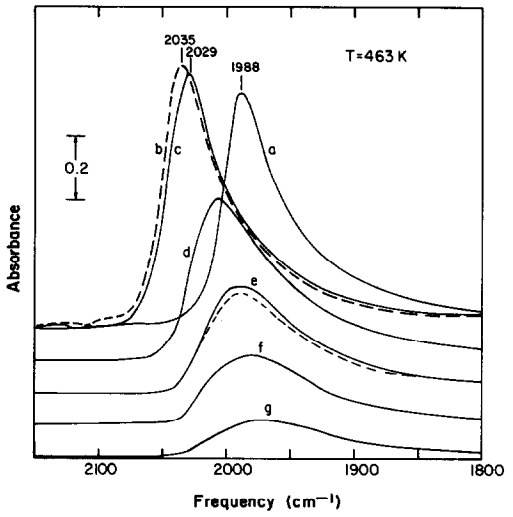

FIG. 6. Infrared spectra of adsorbed CO at successive stages of the experiment shown in Fig. 5: (a) during steady-state reaction in a $^{13}CO/H_2$ mixture (condition B in Fig. 5); (b) after 20 s of contact with a $^{12}CO/H_2$ mixture (condition C in Fig. 5); (c) after 27 s in Ar (condition D in Fig. 5); (d)–(g), at respective times of 47, 107, 167, and 287 s in H_2 (condition A in Fig. 5). Dashed line near spectrum e gives the spectrum at a similar stage in a control experiment using ^{12}CO throughout.

ted in Fig. 5. Production of $^{13}CH_4$ passed through a sharper maximum and prior to that of $^{12}CH_4$ but there was substantial overlap. The quantities of $^{13}CH_4$ and $^{12}CH_4$ produced were 0.9 and 2.8 μmol, respectively.

Infrared spectra recorded at various times in the above experiment are shown in Fig. 6. They confirmed that replacement of adsorbed ^{13}CO by ^{12}CO was complete in the 30 s allowed and that the disappearance of adsorbed ^{12}CO by reaction in H_2 proceeded on a similar time scale to methane production. The dotted line of Fig. 5 shows the estimated rate of loss of adsorbed ^{12}CO as calculated from the spectra by the method described later. It should be stressed that the shift in peak frequency accompanying ^{12}CO removal was solely attributable to the effect of declining coverage and not to ^{13}CO produced by exchange of ^{12}CO with a source of ^{13}C. This may be seen from the close correspondence of spectrum a in Fig. 6 to the adjacent dotted spectrum which was recorded during a control experiment which used ^{12}CO throughout.

Figure 7 shows the results of an experiment similar to that illustrated in Fig. 5 but

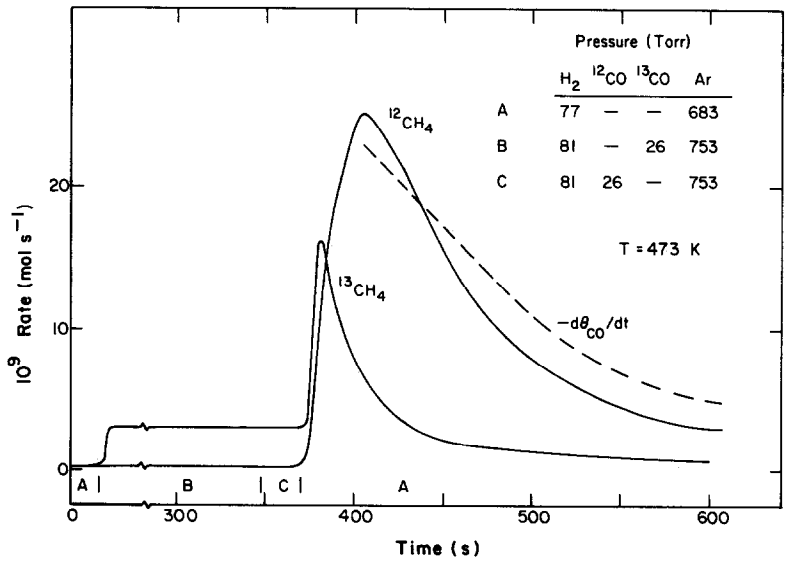

FIG. 7. $^{12}CH_4$ and $^{13}CH_4$ formation and loss of adsorbed ^{12}CO during the sequence $H_2 \rightarrow {}^{13}CO + H_2 \rightarrow {}^{12}CO + H_2 \rightarrow H_2$ at 473 K: Total flow rate = 0.85 STP cm^3/s.

TABLE 3

Estimates for Adsorbed CO and Nonoxygenated Carbon

T (K)	CO/Ru_s[a]	C/Ru_s[a]	$(CO + C)/Ru_s$[a]	Method of determination
498	0.77	0.50	1.27	*b*
463	0.90	0.29	1.19	*c*
473	0.74	0.20	0.94	*d*

[a] In carbon atoms per surface ruthenium atom.

[b] From integrals of transients for CH_4 and H_2O observed in Fig. 4.

[c] From integrals of transients for $^{12}CH_4$ and $^{13}CH_4$ observed in Fig. 5.

[d] From integrals of transients for $^{12}CH_4$ and $^{13}CH_4$ observed in Fig. 7.

at 473 K and without a flushing period in argon. The one significant difference from Fig. 5 was that the peak due to $^{13}CH_4$ was less sharp although its maximum was still reached before that of $^{12}CH_4$. As mentioned in connection with Figs. 4 and 5, this is believed to arise from the inhibition of H_2 adsorption by CO while the latter is being flushed out of the reactor. The amounts of $^{13}CH_4$ and $^{12}CH_4$ produced during the transients shown in Fig. 7 were about 20% lower than the corresponding ones of Fig. 5. While this difference was fairly comparable to the maximum possible error it may be related to the difference in temperature and steady-state exposure time.

Estimates of the amounts of adsorbed CO and nonoxygenated carbon per surface ruthenium atom are presented in Table 3. The determinations of these quantities from the data presented in Figs. 5 and 7 are considered to be more accurate than the estimates obtained from Fig. 4, since in the former case the two carbon sources are resolved isotopically while in the latter the amount of nonoxygenated carbon is determined from the difference in the integrals of the transient responses for CH_4 and H_2O. The data in Table 3 show that under the steady-state conditions used in these experiments the surface of Ru is covered by 80% of a monolayer of adsorbed CO. In addition to this, the catalyst maintains a reservoir of nonoxygenated carbon equivalent to several tenths of a monolayer of Ru. Since the total equivalents of carbon exceeds a monolayer and since there is no evidence from the infrared spectra for diadsorbed CO (*4*), it must be concluded that the nonoxygenated carbon occurs in a form which occupies only a small portion of the ruthenium surface. Two possibilities can be suggested. One is that the carbon exists as thin filaments which are attached to the Ru surface at only a limited number of points. Another possibility is that the carbon spills over from the perimeter of Ru crystallites onto the surface of the support.

Kinetics of Loss of Adsorbed CO

Infrared spectra such as those shown in Fig. 6 were used to assess the rate of loss of adsorbed CO in the presence and absence of H_2. To do so, a linear relationship between integrated band absorbance and CO coverage was assumed. Preliminary measurements (*31*) have shown that this assumption is reasonable for fractional coverages between 0.2 and 0.9. Line a in Fig. 8 shows the net loss of adsorbed CO under argon purge at 473 K following exposure of the catalyst to a CO/H_2 mixture. The apparent first-order rate coefficient associated with this line is 0.7×10^{-3} s^{-1}. The loss of adsorbed CO is much more rapid when H_2 is added to the argon stream. Curve b is observed when the flow of CO is terminated but the flow of H_2 in argon is continued. After a short induction period, the data follow a straight line, characteristic of first-order kinetics. The apparent rate coefficient in this case is 7.2×10^{-3} s^{-1}. Line c shows that purging the reactor with argon for 30 s prior to the introduction of the H_2/Ar stream eliminates the induction period. This is likely due to the removal of gas phase CO which competes with H_2 for adsorption on the ruthenium surface (*2*, *14*). Experiments in which the catalyst was exposed to CO alone gave results identical to

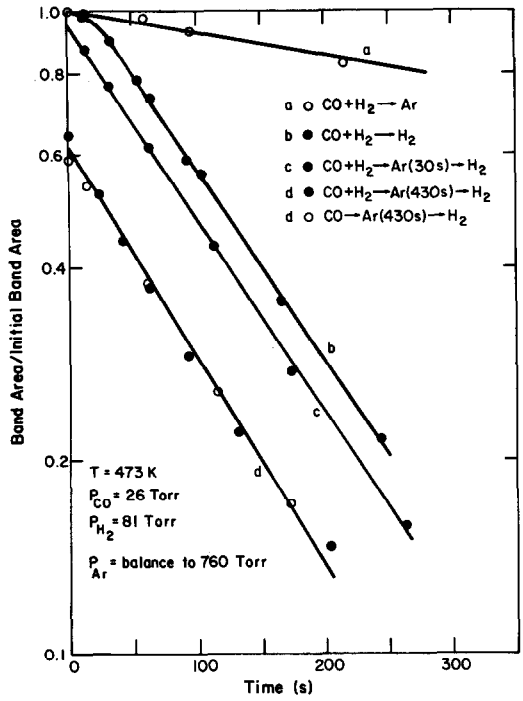

FIG. 8. Plots of CO band area/initial CO band area versus time for removal of adsorbed CO in H_2 at 473 K: Total flow rate = 0.85 STP cm^3/s.

those obtained when exposure was to a CO/H_2 mixture. These data, which appear along line d, show that reduction of the initial CO coverage by extending the period of argon flushing has no effect on the subsequent rate of CO removal in the presence of hydrogen. This observation also suggests that the kinetics of CO removal are first order in CO coverage. Experiments similar to those shown in Fig. 8 were conducted under a variety of conditions to obtain the dependencies of the CO removal rate on H_2 partial pressure and temperature. These results led to a 0.2 order in H_2 partial pressure and an activation energy of 20 kcal/mole.

The loss of adsorbed CO during flushing in argon alone (line a in Fig. 8) can be attributed to the difference in the rates of CO desorption and readsorption. The significance of the latter process can be assessed from the relation (*32*)

$$\frac{r_a}{r_{net}} = \frac{s_0 P(1 - \theta_{CO}) M_{Ru} a_s}{(2\pi mkT)^{1/2} F}, \qquad (2)$$

where r_a is the rate of CO readsorption, r_{net} is the net rate of loss of CO, s_0 is the CO sticking coefficient for CO at zero coverage ($\sim$1.0), P is the total gas pressure in atmospheres, θ_{CO} is the CO coverage, M_{Ru} is the moles of surface Ru atoms in the sample, a_s is the area per surface Ru site ($\sim 10^{-15}$ cm^2), m is the mass of CO, T is the absolute temperature, and F is the total molar flow rate. Evaluation of Eq. (2) for P = 1 atm, $M_{Ru} = 3.86 \times 10^{-6}$ mole, $\theta_{CO} = 0.8$, T = 473 K, and $F = 3.7 \times 10^{-5}$ mole/s gives $r_a/r_{net} = 4.6 \times 10^6$. Consequently, readsorption of CO is seen to be a very significant process even though the CO partial pressure is only about 6×10^{-2} Torr.

The actual rate of desorption can now be estimated as follows. Since

$$r_d/r_{net} = 1 + r_a/r_{net} \qquad (3)$$

then $r_d/r_{net} = 4.6 \times 10^6$. As noted earlier, $r_{net} = 0.7 \times 10^{-3}$ s^{-1} at 473 K. Consequently, $r_d = 3.2 \times 10^3$ s^{-1}. This value of r_d can be compared with that predicted on the basis of results obtained by Pfnür *et al.* (*23*) for CO desorption from a Ru(001) surface. At high CO coverages, the data obtained in that study indicate that the rate coefficient for desorption, k_d, can be described by $k_d \simeq 10^{15} \exp(-25{,}000/RT)(s^{-1})$. Evaluating k_d at 473 K and assuming $\theta_{CO} = 0.8$, leads to $r_d = 2.0 \times 10^3$ s^{-1}. Thus, it is seen that in the present instance there is a close agreement between the rates of CO desorption from Ru/SiO_2 and a Ru(001) surface. The fact that the desorption parameters reported by Pfnür *et al.* (*23*) provide a suitable description here but not for the isotopic exchange experiments reported earlier might possibly be due to the lower surface coverages prevailing during the desorption experiments.

The rate at which adsorbed CO is removed from the surface in the presence of H_2 is much more rapid than the net rate of CO desorption and, as shown in Figs. 5 and 7, closely parallels the rate of methane for-

mation. Since the rate of methane formation from molecularly adsorbed CO is equivalent to the rate of water formation, the rate-limiting step in the formation of both products must be common. The kinetics of CO removal in the presence of H_2 can be represented empirically by

$$\frac{d\theta_{CO}}{dT} = -k_e P_{H_2}^{0.2} \theta_{CO}, \qquad (4)$$

where k_e is the effective rate coefficient. The first-order dependence on CO coverage, appearing in Eq. (4), cannot be rationalized very easily. If CO dissociation is considered to be the rate-limiting step and to proceed as written in reaction (1), for example, then the rate of CO consumption would be proportional to the product of θ_{CO} and the vacancy coverage, θ_v. Assuming an equilibrium coverage by H_2 of the surface not occupied by adsorbed CO then leads to the prediction that the rate of CO depletion should be proportional to $\theta_{CO}(1 - \theta_{CO})/(1 + K_{H_2}^{1/2} P_{H_2}^{1/2})$, where K_{H_2} is the equilibrium constant for H_2 adsorption. Quite obviously the dependencies on CO coverage and H_2 partial pressure appearing in this expression are inconsistent with those in Eq. (4). A better correspondence between predicted and observed kinetics can be achieved by proposing that CO dissociation is assisted by chemisorbed H atoms. In this case it can readily be shown that the kinetics of CO depletion should be proportional to $\theta_{CO}(1 - \theta_{CO}) K_{H_2}^{1/2} P_{H_2}^{1/2}/(1 + K_{H_2} P_{H_2}^{1/2})$. But here too the dependence on CO coverage is far from that observed. The form of Eq. (4) can be rationalized, if one assumes that CO dissociation is preceded by a slow reorientation of the molecule at its point of adsorption (e.g., from perpendicular to parallel with respect to the metal surface) and that this process is accelerated in some fashion by the adsorption of H_2.

Mode of Formation of Carbonaceous Deposits

Experiments comparing transient methane formation in H_2 following periods of exposure to CO and H_2 or to CO alone were made to ascertain the role of H_2 in forming carbonaceous deposits. At temperatures around 498 K or above, no difference was observable following prior exposures varying from 30 s to 30 min. It should be pointed out that any difference in the shape of the transient out to 3 min in H_2 would have been noticeable but differences beyond that time would not have been discernable since the intensity of the peaks in the mass spectrometer was then approaching the background level. For short exposures at lower temperatures significant differences were observed as can be seen from Fig. 9. In the left half of this figure transient methane formation during the sequence CO → Ar (30 s) → H_2, curve a, is seen to lack the sharp initial spike which we associate with hydrogenation of carbonaceous material, which can be seen in curve b, for the sequence CO + H_2 → Ar (30 s) → H_2. Longer argon flushing periods resulted in increasingly larger initial spikes regardless of whether prior exposure was to CO and H_2 or to CO alone. However, their magnitude for the former situation invariably exceeded that for the latter, as may be seen from the right-hand side of Fig. 9. Thus, the presence of the H_2 with CO accelerated the laying down of carbonaceous material in agreement with observations reported previously by Ekerdt and Bell (*2*). This presumably arose by removal of oxygen atoms, formed by CO dissociation, by their conversion to water.

Possible Presence of Hydrogen in the Carbonaceous Layer

Attempts were made to determine if the carbonaceous layer contained hydrogen by employing sequences such as $C^{18}O + H_2 \rightarrow$ Ar(30 s) → D_2. The purpose in using $C^{18}O$ was to shift the mass spectral peaks due to product water out of the region m/e = 17–19, where those due to partially deuterated methanes would reside. These experiments and those of the reverse type, $C^{18}O + D_2 \rightarrow$ Ar(30 s) → H_2, invariably showed that mixed methanes (CH_nD_{4-n}, n = 1–3) were

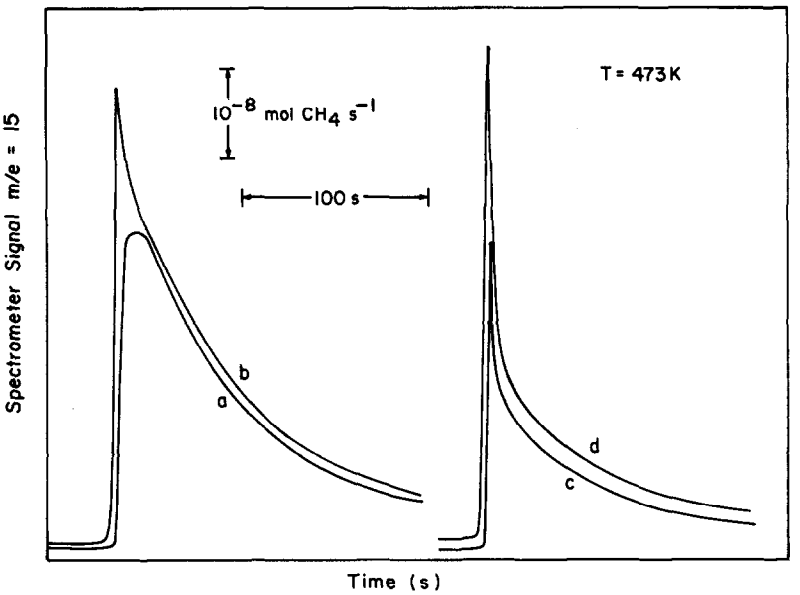

FIG. 9. Transient formation of methane at 473 K in H_2 following exposure to CO + H_2.

produced during the transient stage but HD was always present as well in amounts up to 8% of the D_2. The presence of HD probably arose from exchange of residual water held on the support by the reaction

$$H_2O + D_2 \rightarrow HDO + HD$$

taking place on the metal (*33*). The alternative exchange of surface hydroxyl groups with D_2 was slower. The only possible situation which the experiments did rule out was one in which the sole hydrocarbon moieties present were methyl groups *not* in equilibrium with surface H atoms. In that situation the sequence $C^{18}O + D_2 \rightarrow Ar \rightarrow H_2$ would be expected to produce some CD_3H during the initial phase of the transient, whereas only CH_4, CH_3D, and, in much smaller amounts, CH_2D_2 were found. More informative experiments of the above type may be possible using ruthenium on a low-surface-area support or unsupported ruthenium alone.

Relevance of the Present Results to the Steady-State Synthesis of Methane

Bell and co-workers (*2, 13, 14, 26*) have recently proposed that the synthesis of methane over Ru proceeds via the dissociation of molecularly adsorbed CO and the subsequent hydrogenation of the atomic carbon produced thereby. A steady-state rate expression, which closely corresponds to that observed experimentally, can be derived from this mechanism provided the following assumptions are invoked:

1. Molecularly adsorbed CO is the dominant surface species and is in equilibrium with gaseous CO.
2. The dissociation of molecularly adsorbed CO is reversible and at equilibrium.
3. Dissociative adsorption of H_2 is reversible at equilibrium.
4. Atomic oxygen produced via CO dissociation is rapidly removed as H_2O.
5. Atomic carbon produced via CO dissociation is rapidly hydrogenated to produce CH_x (x = 1–3) species which are in equilibrium with each other.
6. The rate-limiting step in methane formation is the reaction of CH_3 groups with atomic hydrogen.

The present results strongly support a number of the assumptions listed above. First, the infrared and isotopic exchange studies confirm that adsorbed CO is the

major surface species ($\theta_{CO} > 0.85$) and that the exchange of CO between the gas phase and the Ru surface occurs much more rapidly than the steady-state rate of methanation. As a consequence, the assumption that gaseous and adsorbed CO are at equilibrium is reasonable. Second, the formation of nonoxygenated carbon is seen to require surface vacancies (Fig. 9) from which it may be concluded that this form of carbon is produced via CO dissociation. The reversibility of this process is indicated by the occurrence of isotopic scrambling between $^{13}C^{16}O$ and $^{12}C^{18}O$. While it is recognized that the rate of scrambling is much lower than the steady-state rate of methanation, this does not necessarily imply that the rates of dissociation and recombination are slow. As indicated earlier, the limited degree of scrambling observed could be accounted for by slow surface diffusion of atomic carbon and oxygen. Third, the equilibrium scrambling of H_2 and D_2, under synthesis conditions, indicates that the dissociative adsorption of hydrogen is indeed at equilibrium.

A further point brought out by the present work is that while the catalyst maintains a substantial inventory of nonoxygenated carbon, the inventory of atomic oxygen is undetectable. This suggests that atomic oxygen is removed from the Ru surface much more rapidly than carbon. These studies also demonstrate that the nonoxygenated carbon undergoes hydrogenation more readily than adsorbed CO. However, since the consumption of the latter species to form methane begins with only a short delay, one must conclude that the dissociation of CO is a relatively rapid process, in agreement with the earlier results of Biloen *et al.* (*6*).

ACKNOWLEDGMENT

This work was supported by the Director, Office of Energy Research, Office of Basic Energy Sciences, Chemical Sciences Division of the U.S. Department of Energy, under Contract W-7405-ENG-48.

REFERENCES

1. Dalla Betta, R. A., and Shelef, M., *J. Catal.* **48,** 111 (1977).
2. Ekerdt, J. G., and Bell, A. T., *J. Catal.* **58,** 170 (1979).
3. King, D. L., *J. Catal.* **61,** 77 (1980).
4. Kellner, C. S., and Bell, A. T., *J. Catal.* **71,** 296 (1981).
5. Rabo, J. A., Risch, A. P., and Poutsma, M. L., *J. Catal.* **53,** 295 (1978).
6. Biloen, P., Helle, J. N., and Sachtler, W. M. H., *J. Catal.* **58,** 95 (1979).
7. Biloen, P., *J. R. Neth. Chem. Soc.* **99,** 33 (1980).
8. Low, G. G., and Bell, A. T., *J. Catal.* **57,** 397 (1979).
9. Araki, M., and Ponec, V., *J. Catal.* **44,** 439 (1976).
10. Wentrcek, P. R., Wood, B. J., and Wise, H., *J. Catal.* **43,** 363 (1976).
11. Dalla Betta, R. A., and Shelef, M., *J. Catal.* **49,** 383 (1977).
12. Wilson, T. P., *J. Catal.* **60,** 167 (1979).
13. Kellner, C. S., and Bell, A. T., *J. Catal.* **67,** 175 (1981).
14. Kellner, C. S., and Bell, A. T., *J. Catal.* **70,** 418 (1981).
15. Savatsky, B. J., and Bell, A. T., *ACS Symp. Ser* **178** (1982).
16. Hicks, R. F., Kellner, C. S., Savatsky, B. J., Hecker, W. C., and Bell, A. T., *J. Catal.* **71,** 216 (1981).
17. Hammaker, R. A., Francis, S. A., and Eischens, R. P., *Spectrochim. Acta* **21,** 1295 (1965).
18. Crossley, A., and King, D. L., *Surf. Sci.* **68,** 528 (1977).
19. Crossley, A., and King, D. L., *Surf. Sci.* **95,** 131 (1980).
20. Klier, K., Zettlemoyer, A. C., and Leidheiser, H., Jr., *J. Chem. Phys.* **52,** 589 (1970).
21. Yates, J. T., Jr., Duncan, T. M., and Vaughn, R. W., *J. Chem. Phys.* **71,** 3908 (1979).
22. Yates, J. T., Jr., and Goodman, D. W., *J. Phys. Chem.* **73,** 5371 (1980).
23. Pfnür, H., Feulner, P., ENglehardt, H. A., and Menzel, D., *Chem. Phys. Lett.* **59,** 481 (1978).
24. Pfnür, H., Menzel, D., Hoffman, F. M., Ortega, A., and Gradshaw, A. M., *Surf. Sci.* **93,** 431 (1980).
25. Bossi, A., Carnisio, G., Garbassi, F., Giunchi, G., Petrini, G., and Zanderighti, L., *J. Catal.* **65,** 16 (1980).
26. Bell, A. T., *Catal. Rev. Sci. Eng.* **23,** 203 (1981).
27. Ozaki, A., "Isotopic Studies of Heterogeneous

Catalysis." Academic Press, New York, 1977.
28. Dalla Betta, R. A., Piken, A. G., and Shelef, M., *J. Catal.* **35,** 54 (1974).
29. Vannice, M. A., *J. Catal.* **37,** 449 (1975).
30. Vannice, M. A., *J. Catal.* **37,** 462 (1975).
31. Winslow, P., Cant, N., and Bell, A. T., unpublished results.
32. Savatsky, B. J., Ph.D. thesis, Department of Chemical Engineering, University of California, Berkeley, Calif. 94720.
33. Sargert, N. H., and Pouteau, R. M. L., *Canad. J. Chem.* **51,** 4031 (1973).